Original Article

Comparison of ultrasound and magnetic resonance imaging of the median nerve's recurrent motor branch and the value of its diameter in diagnosing carpal tunnel syndrome

Yeting Wang, Wen Chen, Tiezheng Wang, Kezhen Qin, Jianbo Teng, Hengtao Qi^

Department of Ultrasound, Shandong Provincial Hospital Affiliated to Shandong First Medical University, Jinan, China

Contributions: (I) Conception and design: H Qi, Y Wang; (II) Administrative support: J Teng; (III) Provision of study materials or patients: H Qi, T Wang; (IV) Collection and assembly of data: Y Wang, W Chen; (V) Data analysis and interpretation: Y Wang, K Qin; (VI) Manuscript writing: All authors; (VII) Final approval of manuscript: All authors.

Correspondence to: Hengtao Qi, MD. Department of Ultrasound, Shandong Provincial Hospital Affiliated to Shandong First Medical University, No. 324, Jingwu Road, Jinan 250021, China. Email: elementfe@126.com.

Background: Anatomical variations of the recurrent motor branch (RMB) are at risk of injury during carpal tunnel release procedures. Previous studies have visualized the RMB using ultrasound (US) and magnetic resonance imaging (MRI) but have not compared the imaging capabilities of the two. Previous investigations have overlooked two specific types of carpal tunnel syndrome (CTS): simultaneous compression of the median nerve and the RMB and isolated compression of the latter. This study aims to identify the best imaging method to prevent iatrogenic injury to the RMB by comparing US and MRI capabilities. It also aims to devise a new method for the comprehensive diagnosis of CTS by evaluating the initial diameter of the RMB (RMB-ID). Additionally, this study aims to gain insights into the distribution patterns of the different anatomic variations of the RMB in healthy individuals and patients through an analysis of these variations. A cross-sectional study was conducted.

Methods: Forty healthy adults subjected to bilateral US and MRI of the RMB were included in this study. The US and magnetic resonance images of each patient were subsequently compared. US imaging of the RMB was performed on 102 hands of healthy adults and 112 hands of patients with CTS. The cross-sectional area of the median nerve (MN-CSA) and RMB-ID were measured.

Results: US provided better visibility of the RMB than did MRI (P<0.05). No statistically significant difference was observed in the variation type composition of the RMB between the healthy and patient groups (P>0.05). The RMB-ID and the MN-CSA significantly differed between groups (P<0.001). The RMB-ID increased with the increase of the MN-CSA (R=0.842; P<0.001). The optimal cutoff point for diagnosing CTS of the RMB-ID was 0.85 mm, yielding a sensitivity of 83.0%, a specificity of 92.2%, and the area under the curve of 0.945. The MN-CSA was 0.115 cm^2, with a sensitivity of 73.2%, a specificity of 96.1%, and an area under the curve of 0.923 [95% confidence interval (CI): 0.887–0.958]. No statistically significant difference was observed in the area under the receiver operator characteristic curve between the two diagnostic methods (P>0.05). The interexaminer reliability for the RMB-ID and the MN-CSA measurements was 0.983 (95% CI: 0.978–0.987) and 0.966 (95% CI: 0.955–0.974), respectively.

Conclusions: US outperformed MRI in visualizing the anatomical variations of the RMB. The RMB-ID was an accurate and valid indicator for comprehensive diagnosis of CTS.

^ ORCID: 0000-0002-2834-3246.

Keywords: Carpal tunnel syndrome (CTS); diagnostic imaging; magnetic resonance image; ultrasonography; recurrent motor branch (RMB)

Submitted Jul 10, 2024. Accepted for publication Oct 01, 2024. Published online Dec 30, 2024.
doi: 10.21037/qims-24-1410
View this article at: https://dx.doi.org/10.21037/qims-24-1410

Introduction

The diagnosis of carpal tunnel syndrome (CTS) is typically based on clinical symptoms and physical examination and is confirmed by nerve conduction study (NCS) (1). However, NCS can cause discomfort to patients during the examination. The results of a prospective study (2) comparing the clinical and electrical diagnosis of CTS indicated that NCS demonstrated high sensitivity (94%) and positive predictive value (87%) but low specificity (50%). Thus, NCS may be more suited to ruling out rather than confirming a diagnosis of CTS (3). Ultrasound (US) is considered the preferred imaging modality for diagnosing CTS (4). The advantages of US over NCS are that it is noninvasive, can visualize the anatomical features of the median nerve and its surrounding tissue, can differentiate between primary and secondary CTS, can visualize the underlying cause of secondary CTS, and can provide information for surgical intervention (5-7). The results of a meta-analysis comparing the sensitivity and specificity of US and NCS in diagnosing CTS suggested that while US may not replace NCS, it can be considered as a viable alternative to NCS as a first-line diagnostic test (8). Most ultrasonographic studies have collected images of the transverse section at the inlet level to the transverse carpal ligament and measured the cross-sectional area of the median nerve (MN-CSA) to identify the amount of median nerve enlargement (9,10). However, identifying and tracing the irregular surface using this approach may be challenging in some cases (11). One drawback of this approach is its failure to detect two special types of CTS: combined compression of the median nerve and recurrent motor branch (RMB) and isolated RMB compression (or represent a distinct entity) (12). Furthermore, NCS has a very low sensitivity for the diagnosis of motor nerve damage such as RMB (13). Therefore, we propose a novel diagnostic approach for CTS, which uses the measurement of the initial diameter of the RMB (RMB-ID). Typically, after exiting the carpal tunnel, the median nerve bifurcates into the medial and lateral branches (14). The lateral branch branches out the RMB, which supplies motor innervation to the opponens pollicis, the abductor pollicis brevis, and the superficial portion of the flexor pollicis brevis (14). Our proposed method enables accurate diagnosis of isolated median nerve compression and of the two special types of CTS mentioned above. As discerned on US images, the nerve usually flattens out at compression site, and swelling occurs proximal and distal to this point, so when the median nerve is compressed, the RMB—the largest branch of the wrist—becomes swollen and thickened (15,16). Additionally, injury to the RMB during carpal tunnel release is also referred to as a million dollar injury (17,18). The susceptibility of the RMB to iatrogenic damage can be attributed to its anatomical variations. The risk of iatrogenic injury increases with the more medial origin of the recurrent branch from the median nerve and a greater angle of origin (19). Poisel *et al.* classified RMB branching into three types according to the location and relationship to the transverse carpal ligament: extraligamentous (type I), subligamentous (type II), and transligamentous (type III) (20). The transligamentous type of RMB is associated with a particularly high risk of injury during carpal tunnel release (21).

In order to prevent iatrogenic injury of the RMB, this study employed an optimal preoperative imaging examination to assess the anatomical variations of the RMB prior to surgery. Consequently, a comparative analysis was conducted between US and magnetic resonance imaging (MRI) in terms of their ability to visualize the RMB of the median nerve. Additionally, for a comprehensive and reliable diagnosis of CTS, the diagnostic value of RMB-ID measured on US images was compared with that of MN-CSA measured on axial US images. We present this article in accordance with the STROBE reporting checklist (available at https://qims.amegroups.com/article/view/10.21037/qims-24-1410/rc).

Methods

Study approval

The study was conducted in accordance with the Declaration of Helsinki (as revised in 2013) and was approved by the Ethics Committee of Shandong Provincial Hospital Affiliated to Shandong First Medical University (approval No. MR-37-23-023994). Informed consent was obtained from all participants.

The comparative evaluation of US and MRI for RMB visualization

Participant selection

Forty healthy volunteers from our ultrasound department's refresher doctor and hospital staff were recruited between September and October 2023. Patients with median never diseases outside the wrist such as cervical spondylosis, brachial plexus injury, Struthers' ligament compression, pronator teres syndrome, neuritis, median nerve injury, or neuroma were excluded. Clinical information collected included age and sex.

US and MRI examination

An Aplio i800 US machine (Canon Medical Systems, Otawara, Japan) equipped with a L24 linear array transducer (i24LX8; Canon Medical Systems) was used in our study. The scans were acquired and evaluated by a musculoskeletal radiologist (H.Q.) with more than 10 years of practical experience. For US examination, the patients were seated in a chair positioned opposite the table, with their hands outstretched, wrists supinated, and fingers relaxed. The MN-CSA was systematically examined from its entry into the carpal tunnel (at the level of the pisiform bone) to its distal end, with particular attention given to the tracking of the tubular structure originating from the median nerve and extending toward the thenar muscle. The origin and movement of the RMB were subsequently assessed via rotation of the probe. The beam angle and direction were adjusted so that the beam was as perpendicular as possible to the RMB, which could help clearly display the RMB and avoid anisotropic artifacts. Subsequently, the RMB was tracked until it entered the thenar major muscle group. To ensure distinction from the palmar cutaneous branch or palmar digital branch of the median nerve, entry into the thenar major muscle is essential for identification of RMB. Color Doppler was employed to avoid confusion with blood vessels.

MRI scanning was performed on a 3-T MRI scanner (MAGNETOM Vida, Siemens Healthineers, Erlangen, Germany) with an 18-channel flexible coil. For MRI examination, the patient was placed in a supine position with the hands naturally at the side of the body and the palms facing upward for imaging. Scans included T1-weighted turbo spin echo (T1-TSE) [repetition time (TR), 580 ms; echo time (TE), 11 ms; flip angle (FA), 110°; number of excitations: 6, voxel size, 0.39 mm × 0.31 mm × 2.0 mm; acquisition time (AT), 3 minutes and 3 seconds] and proton density-weighted turbo spin echo (PD-TSE) (TR, 2,620 ms; TE, 21 ms; FA, 110°; voxel size, 0.39 mm × 0.31 mm × 1.5 mm; number of excitations: 8; AT, 4 minute and 50 seconds).

A series of assessments of the anatomical variations of the RMB were performed on both US and MRI images, including the location of the RMB's origin from the median nerve (radialis, medialis, and ulnar), its angle to the median nerve (0°, 30°, 60°, and 90°), and the Poisel classification of the RMB. The visibility of the RMB was graded using a five-point scale as follows (22): excellent—sharply defined border and visible internal nerve structure with excellent diagnostic quality; good—good diagnostic quality, clearly distinguishable from surrounding tissue, and internal nerve structure visible; moderate—identifiable, but no sharp border from surrounding tissue and no internal nerve structure visible; poor—difficulty in identification or only possible if followed by adjacent nerve sections; and not visible.

Evaluation on the diagnostic value of recurrent branch diameter in CTS

Participant selection

We examined patients diagnosed with bilateral CTS at the outpatient clinic between August 2023 and February 2024. The CTS group consisted of 112 hands from 56 patients (44 women and 12 men). We selected 102 hands from 51 patients who attended Shandong Provincial Hospital Affiliated to Shandong First Medical University and were diagnosed with other diseases to form a control group (35 women and 16 men). The age and gender of the control group and the CTS group were matched. The demographic data of the patients in the CTS and control groups are shown in *Table 1*.

The inclusion and exclusion criteria for patients with CTS are shown in *Figure 1* (23).

Table 1 Baseline demographic data of the study participants

Variables	Healthy volunteers (n=51, 102 wrists)	Patients with CTS (n=56, 112 wrists)	P value
Age (years)	46 [39–50]	49 [36–57]	0.456
Sex			0.242
Female	35	44	
Male	16	12	

Data are presented as median [interquartile range] or number. CTS, carpal tunnel syndrome.

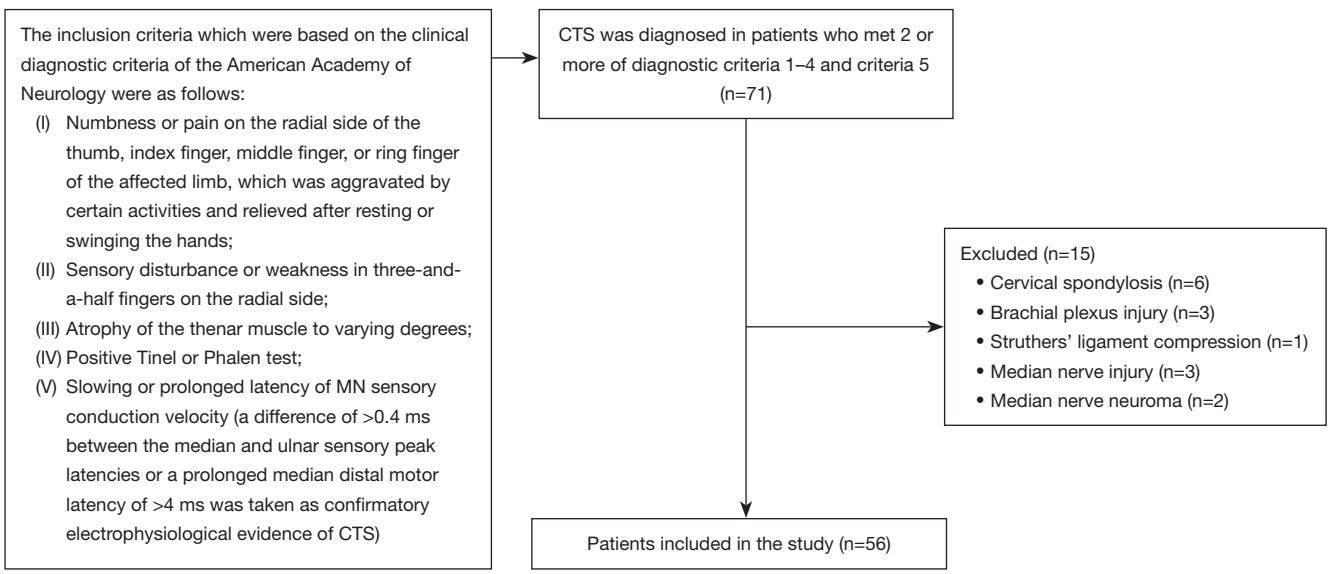

Figure 1 Flowchart of the inclusion of patients with CTS in this study. CTS, carpal tunnel syndrome; MN, median nerve.

US examination

The US scans were independently acquired by a musculoskeletal radiologist (H.Q.) with more than 10 years of practical experience and a musculoskeletal radiologist (T.W.) with more than 5 years of practical experience. The US equipment and examination methods were the same as those described above. The two musculoskeletal radiologists conducted the examination without prior knowledge of the clinical symptoms or NCS results.

Statistical analyses

Statistical analysis was performed using SPSS version 27.0.1 (IBM Corp., Armonk, NY, USA). The quantitative data are expressed as mean ± standard deviation (SD), while enumeration data are expressed as constituent ratio or rate (%). A Pearson Chi-squared test was used to evaluate the comparison of the visibility of the anatomical variations of the RMB on US and MRI and the gender composition between the two groups. The Fisher exact test was conducted to statistically compare the composition of RMB types between the healthy and patient groups. The Shapiro-Wilk test was used for normally distributed data. Comparisons between the healthy and patient control groups were performed using the Student's *t*-test or the Mann-Whitney test after the normality of MN-CSA, RMB-ID, and age in patients was assessed. The relationship between RMB-ID and MN-CSA was analyzed via simple linear regression. To estimate the relative diagnostic accuracy of the RMB-ID and MN-CSA, the sensitivity and specificity were calculated, and a receiver operating characteristic (ROC) curve was used to estimate the optimal cutoff values. The diagnostic value of MN-CSA and RMB-ID was compared with the DeLong test. The interexaminer reliability for ultrasonographic measurements was examined using the intraclass correlation coefficient (ICC) (1,2).

Table 2 Comparison of the visualization of the RMB between US and MRI

Imaging method	Excellent	Good	Moderate	Poor	Not visible	P value
US	9	42	25	4	0	<0.05*
MRI	4	28	33	8	7	

*, statistically significant difference. RMB, recurrent motor branch; US, ultrasound; MRI, magnetic resonance imaging.

Table 3 RMB variation type for the patients with CTS and healthy volunteers

Variation type	Healthy volunteers	Patients with CTS	P value
IA	29	25	>0.05
IIA	0	1	
IIIA	0	0	
IB	12	21	
IIB	6	2	
IIIB	0	1	
IC	14	13	
IIC	6	4	
IIIC	0	0	
ID	23	32	
IID	12	13	
IIID	0	0	

The recurrent branch originates from the radial, middle, and ulnar regions of the median nerve, which correspond to the Roman numerals I–III, respectively, and the angles of 0°, 30°, 60°, and 90°, with the axis plane of the median nerve corresponding to the letters A–D, respectively. RMB, recurrent motor branch; CTS, carpal tunnel syndrome.

Table 4 Ultrasonographic measurements of the RMB-ID and MN-CSA in the patients with CTS and healthy volunteers

Group	N	RMB-ID (mm)	MN-CSA (cm^2)	P value
Healthy volunteers	102	0.7 [0.7–0.8]	0.09 [0.08–0.10]	<0.001*
Patients with CTS	112	1.0 [0.9–1.2]	0.18 [0.11–0.27]	<0.001*

Data are presented as median [interquartile range]. *, statistically significant difference. RMB-ID, initial diameter of the recurrent motor branch; MN-CSA, cross-sectional area of the median nerve; CTS, carpal tunnel syndrome.

Results

The visibility of the RMB showed a statistically significant difference between US and MRI, with US demonstrating significantly superior results compared to MRI (*Table 2*). There was no significant difference in the age or sex ratio between the healthy group and the patient group (*Table 1*). There was no statistically significant difference observed in the variation-type composition of the RMB between the healthy and patient groups (*Table 3*). The MN-CSA and RMB-ID in the patient group were significantly higher than those in the healthy group (*Table 4* and *Figure 2*). A significant linear relationship was observed between the two variables, with RMB-ID increasing as MN-CSA increased, and the regression coefficient was 0.842 (*Figure 3*). ROC curve analysis indicated that the optimal cutoff point for diagnosing CTS of RMB-ID was 0.85 mm, with a sensitivity of 83.0%, a specificity of 92.2%, and an area under the curve of 0.945 (95% CI: 0.917–0.972);

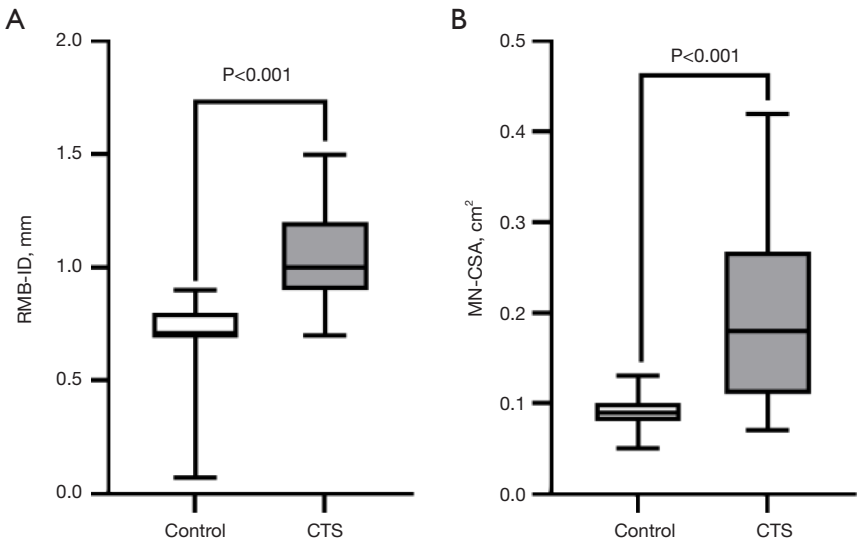

Figure 2 Distribution of the RMB-ID and MN-CSA in the CTS and control groups. (A) Distribution of the RMB-ID. (B) Distribution of the MN-CSA. RMB-ID, initial diameter of the recurrent motor branch; MN-CSA, cross-sectional area of the median nerve; CTS, carpal tunnel syndrome.

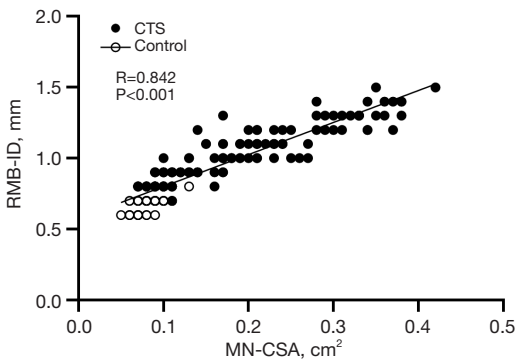

Figure 3 Regression plots between MN-CSA and RMB-ID. A strong correlation was found between the MN-CSA and RMB-ID in patients with CTS (R=0.842; P<0.001). MN-CSA, cross-sectional area of the median nerve; RMB-ID, initial diameter of the recurrent motor branch; CTS, carpal tunnel syndrome.

meanwhile, the optimal cutoff point for diagnosing CTS of MN-CSA was 0.115 cm^2, with a sensitivity of 73.2%, a specificity of 96.1%, and an area under the curve of 0.923 (95% CI: 0.887–0.958) (*Figure 4*). There was no statistical difference in the area under ROC curve between RMB-ID and MN-CSA in diagnosing CTS (*Table 5*). The inter examiner reliability for the RMB-ID and MN-CSA measurements was 0.983 (95% CI: 0.978–0.987) and 0.966 (95% CI: 0.955–0.974), respectively.

Discussion

This study compared the imaging capabilities of US and MRI for RMB. In addition, the diagnostic value of the RMB-ID in CTS was examined. The visualization of the RMB on US was superior to that on MRI, and RMB-ID demonstrated excellent diagnostic value in the evaluation of CTS. To the best of our knowledge, this is the first study to demonstrate that US is superior to MRI for RMB imaging and that RMB-ID has excellent diagnostic value for CTS.

Surgical intervention is often necessary following RMB injury; however, clinical symptoms may not be immediately apparent due to the pure motor function of the RMB. In the early stages after injury, patients may only experience muscle contraction weakness without pain or numbness, leading to delayed medical treatment until more obvious symptoms such as thumb and palm restriction and decline in thumb pinch strength, along with muscle atrophy, occur (24,25). Moreover, the efficacy of delayed repair remains uncertain (26). *Figure 5* provides a representative case of iatrogenic injury to the RMB in a 58-year-old female patient, who developed atrophy of the thenar muscles following CTS release. Ultrasonography findings indicated rupture of the RMB. On ultrasonic images, the normal RMB appears as a tubular hypoechoic structure surrounded by a hyperechoic epineurium (*Figure 6*). On MRI, the normal RMB appears as a strip-like structure with signal

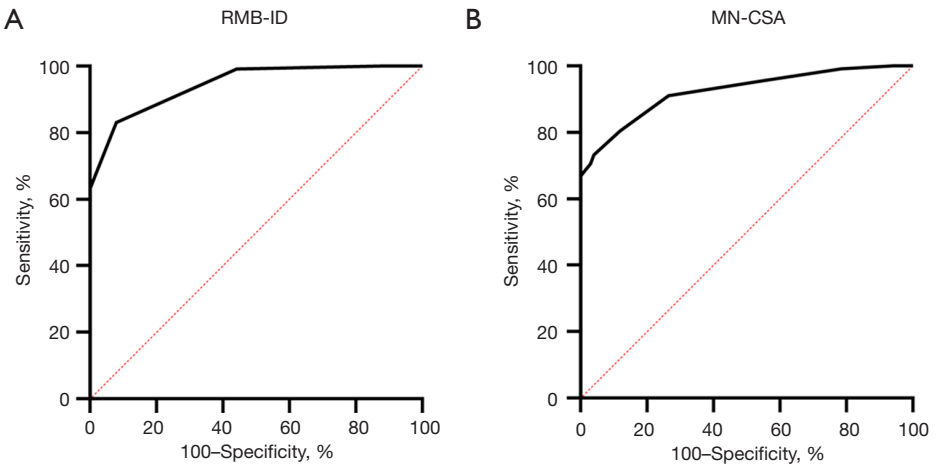

Figure 4 The receiver operating characteristic curve analysis for diagnosing CTS. (A) RMB-ID. (B) MN-CSA. CTS, carpal tunnel syndrome; RMB-ID, initial diameter of the recurrent motor branch; MN-CSA, cross-sectional area of the median nerve.

Table 5 DeLong test for area under the ROC curve of RMB-ID and MN-CSA

Variables	AUC (95% CI)	P value
RMB-ID	0.945 (0.917–0.972)	0.133
MN-CSA	0.923 (0.887–0.958)	

ROC, receiver operating characteristic; RMB-ID, initial diameter of the recurrent motor branch; MN-CSA, cross-sectional area of the median nerve; AUC, area under the ROC curve; CI, confidence interval.

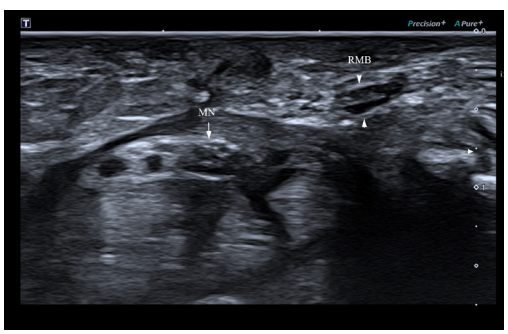

Figure 5 In the image, RMB is interrupted at its origin from the MN, and the severed end of the RMB shows tumor-like dilatation. The short arrows indicate the stump of the RMB. The long arrow indicates the short axis of the MN. RMB, recurrent motor branch; MN, median nerve.

intensities equal to or slightly higher than those of the surrounding muscles (*Figure* 7). US enabled determination of the Poisel type and precise identification of the position and angle at which the RMB originates from the median nerve. Although MRI could also visualize similar anatomical variations of RMB as US, its ability to depict RMB was generally inferior. The magnetic resonance neuroimaging technique exhibits certain limitations, such as the occurrence of the magic angle effect (27). Magnetic resonance neurography technology requires a high-field MR scanner to obtain adequate signal-to-noise ratio and very fine spatial resolution (28). However, high-field MR scanners can significantly compromise image quality (29,30). Although curved multiplane reconstruction makes it possible to visualize neural structures with tortuous courses or oblique orientations, nerve measurement might be susceptible to variability due to asymmetrically curved multiplane reconstruction (7,31). US has some advantages over MRI, including real-time examination capability, reduced scan duration, adjustable inspection field of view based on clinical indications, and the ability to generate dynamic images for assessing nerve mobility in cases of movement or compression (32). The healthy side can serve as a control in US examination for unilateral diseases, thereby enhancing the detection of subtle nerve and muscle

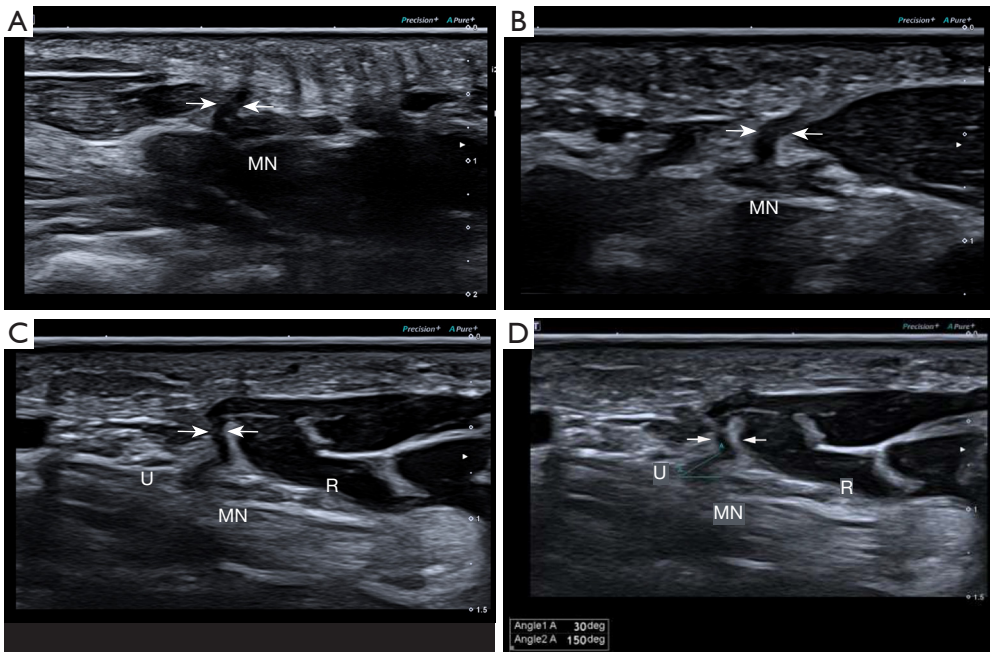

Figure 6 The location and angle of the RMB originating from the MN. (A-C) The RMB originating from different locations of the MN. (A) The RMB originating from the radial aspect of the MN. (B) The RMB originating from the medial aspect of the MN. (C) The RMB originating from the ulnar aspect of the MN. (D) An angle between the RMB and the MN axis plane of 30°. The arrows indicate the long axis of the RMB. RMB, recurrent motor branch; R, the radial side of the palm; U, the ulnar side of the palm; MN, median nerve.

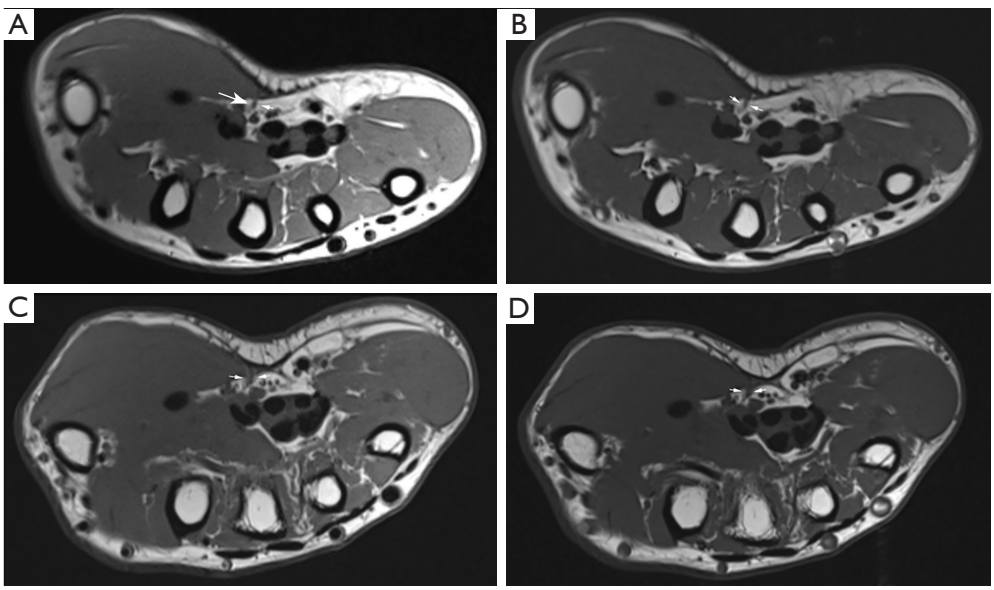

Figure 7 Magnetic resonance imaging of the RMB. (A,C) Cross-sectional proton density-weighted images. (B,D) Cross-sectional T1-weighted images. (A,B) A case in which the RMB visibility was rated as excellent. (C,D) A case in which the RMB visibility was rated as moderate. The arrows indicate the long axis of the RMB. RMB, recurrent motor branch.

abnormalities (33). The use of the color Doppler technique aids in the differentiation of the regional vasculature for small peripheral nerves (34). Moreover, US offers enhanced spatial resolution and facilitates the provision of more precise information regarding the extent of nerve involvement, can demonstrate tiny peripheral nerves that may not be visible on MRI, and can better guide hand surgeons in the selection of a suitable surgical approach (35-37). In addition, research suggests that high-resolution US is capable of imaging the RMB and discerning the anatomical variations of the RMB and the morphological changes associated with its pathological conditions (38-40). However, previous studies did not use US to quantify the angle of origin for RMB from the median nerve, nor did they examine the risk type of iatrogenic injury of RMB. In our study, we integrated the Poisel type system for RMB and conducted statistical analysis on the types of iatrogenic injury risks of RMB based on both the location and angle of the RMB origin from the median nerve (19,20). There was no significant difference in the composition of different types of RMB between healthy individuals and patients. The most common anatomical variation types observed were IA, IB, IC, ID, and IID. Among these variations, type IA exhibited greater safety during carpal tunnel release procedures while type IID demonstrated a higher susceptibility to iatrogenic injuries. Poisel type of RMB in all participants was extraligamentous, which may be related to our small sample size or the nationality of participants. The anatomical variations of all the RMB we examined were in accordance with those observed intraoperatively in patients who had undergone surgery.

MN-CSA and RMB-ID in the CTS patient group were significantly higher than those in the healthy control group, and the average RMB-ID in the healthy control group was 0.7 mm, which aligns with findings from recent studies conducted in the United States and Italy using high-frequency US for RMB-ID measurement (40,41). Moreover, the increase in RMB-ID being associated with the increase in MN-CSA is also consistent with the results of a recently published study, which also reported that the difference in the location of median nerve compression, the difference in the thickness of flexor retinaculum, and the presence of flexor tendons tenosynovitis do not affect the degree of RMB swelling (41).

The compression of the nerve is followed by a breakdown of the blood–nerve barrier, subperineurial edema and fibrosis at the compression site, and finally edema and diffuse proximal and distal fibrosis (42). With increased time of compression, the large myelinated fibers undergo segmental demyelination, which is initially localized at the site of compression and then diffuses both proximally and distally (42). The primary form of nerve injury in CTS is characterized by demyelination (42). Therefore, edema and demyelination of the median nerve due to compression will affect its largest branch in the wrist, the RMB. The demyelination of the RMB can be diagnosed by an increase in its diameter on US imaging. This diagnostic approach was further supported by our calculation of an area under the ROC curve (0.945). For the first time, we identified 0.85 mm as the RMB-ID cutoff value for diagnosing CTS. Compared with MN-CSA, the diagnostic specificity of RMB-ID was slightly lower, but the sensitivity was higher than that of MN-CSA. Notably, there were no statistically significant differences observed between RMB-ID and MN-CSA in their ability to diagnose CTS.

The double crush hypothesis was first proposed over 50 years ago (43). It holds that compression of the nerve at its proximal end renders it more susceptible to compression at multiple sites along its distal end; the greater likelihood of compression of the distal nerve makes the already compressed nerve at the proximal end more vulnerable to secondary compression, resulting in a reverse double compression (43). The compression of one side of the median nerve or RMB increases the likelihood of compression on the other side. Therefore, we propose a new indicator for the diagnosis of CTS, RMB-ID, which cannot only reflect the extent of median nerve compression but also avoid missing two special types of CTS. These special types include simultaneous compression of both the median nerve and RMB and isolated compression solely affecting the RMB (or in lieu of a separate entity). Examples of this include RMB compression due to schwannomas (44-46), ganglia (47-49), anomalous anatomical structures (50,51), long distance cycling (52), or cutting injuries (53). We believe that this concept of double or multiple crush imbues the measurement and examination of the RMB of patients with both median nerve and RMB compression with clinical significance, as failure to diagnose and treat these injuries simultaneously may result in persistent symptoms for patients.

Our study involved certain limitations which should be addressed. First, we did not record the height and weight of healthy volunteers and patients with CTS. Although, a meta-analysis (54) indicated that MN-CSA is not correlated with height, weight, or body mass index (BMI), some studies (41) suggest the existence of an association between

RMB-ID and BMI. Second, the NCS results of patients with CTS in this study were relatively simple, so we could not classify CTS into mild, moderate, or severe according to the NCS results to compare differences in RMB-ID between groups of different disease severities. Third, we used a hand as an independent sample to maximize the sample size. To avoid overestimation in future studies, it is recommended to use an individual as the sampling unit rather than a hand.

Conclusions

The US imaging capability for RMB surpasses that of MRI, making it the preferred choice for assessing anatomical variations in RMB prior to carpal tunnel release. US can accurately identify risky types of RMB, which can help to avoid iatrogenic injury. RMB-ID is a novel, sensitive, and reliable indicator for the comprehensive diagnosis of CTS.

Acknowledgments

A portion of the manuscript has already been presented at the 16th Congress of the Asian Federation of Societies for Ultrasound in Medicine and Biology in conjunction with KSUM 2024.
Funding: This work was supported by Shandong Provincial Natural Science Foundation, China (No. ZR2022MH043).

Footnote

Reporting Checklist: The authors have completed the STROBE reporting checklist. Available at https://qims.amegroups.com/article/view/10.21037/qims-24-1410/rc

Conflicts of Interest: All authors have completed the ICMJE uniform disclosure form (available at https://qims.amegroups.com/article/view/10.21037/qims-24-1410/coif). The authors have no conflicts of interest to declare.

Ethical Statement: The authors are accountable for all aspects of the work in ensuring that questions related to the accuracy or integrity of any part of the work are appropriately investigated and resolved. This study was conducted in accordance with the Declaration of Helsinki (as revised in 2013) and was approved by the Ethics Committee of Shandong Provincial Hospital Affiliated to Shandong First Medical University (approval No. MR-37-23-023994). Informed consent was obtained from all participants.

References

1. Malakootian M, Soveizi M, Gholipour A, Oveisee M. Pathophysiology, Diagnosis, Treatment, and Genetics of Carpal Tunnel Syndrome: A Review. Cell Mol Neurobiol 2023;43:1817-31.
2. Wang WL, Buterbaugh K, Kadow TR, Goitz RJ, Fowler JR. A Prospective Comparison of Diagnostic Tools for the Diagnosis of Carpal Tunnel Syndrome. J Hand Surg Am 2018;43:833-836.e2.
3. Dahlin LB, Zimmerman M, Calcagni M, Hundepool CA, van Alfen N, Chung KC. Carpal tunnel syndrome. Nat Rev Dis Primers 2024;10:37.
4. Petrover D, Richette P. Treatment of carpal tunnel syndrome : from ultrasonography to ultrasound guided carpal tunnel release. Joint Bone Spine 2018;85:545-52.
5. Deniz FE, Oksüz E, Sarikaya B, Kurt S, Erkorkmaz U, Ulusoy H, Arslan S. Comparison of the diagnostic utility of electromyography, ultrasonography, computed tomography, and magnetic resonance imaging in idiopathic carpal tunnel syndrome determined by clinical findings. Neurosurgery 2012;70:610-6.
6. Dailiana ZH, Bougioukli S, Varitimidis S, Kontogeorgakos V, Togia E, Vlychou M, Malizos KN. Tumors and tumor-like lesions mimicking carpal tunnel syndrome. Arch Orthop Trauma Surg 2014;134:139-44.
7. Purger DA, Sakamuri S, Hug NF, Biswal S, Wilson TJ. Imaging of Damaged Nerves. Clin Plast Surg 2020;47:245-59.
8. Zaki HA, Shaban E, Salem W, Bilal F, Fayed M, Hendy M, Abdelrahim MG, Masood M, Mohamed Khair Y, Shallik NA. A Comparative Analysis Between Ultrasound and Electromyographic and Nerve Conduction Studies in Diagnosing Carpal Tunnel Syndrome (CTS): A Systematic Review and Meta-Analysis. Cureus 2022;14:e30476.
9. Tai TW, Wu CY, Su FC, Chern TC, Jou IM. Ultrasonography for diagnosing carpal tunnel syndrome: a meta-analysis of diagnostic test accuracy. Ultrasound Med Biol 2012;38:1121-8.

10. Torres-Costoso A, Martínez-Vizcaíno V, Álvarez-Bueno C, Ferri-Morales A, Cavero-Redondo I. Accuracy of Ultrasonography for the Diagnosis of Carpal Tunnel Syndrome: A Systematic Review and Meta-Analysis. Arch Phys Med Rehabil 2018;99:758-765.e10.
11. Sonofuchi K, Hatta T, Goto H. Ultrasonographic Measurement of the Median Nerve Transverse Diameter at the Wrist for Diagnosing Carpal Tunnel Syndrome. J Hand Surg Asian Pac Vol 2021;26:223-8.
12. Bennett JB, Crouch CC. Compression syndrome of the recurrent motor branch of the median nerve. J Hand Surg Am 1982;7:407-9.
13. Demino C, Fowler JR. The Sensitivity and Specificity of Nerve Conduction Studies for Diagnosis of Carpal Tunnel Syndrome: A Systematic Review. Hand (N Y) 2021;16:174-8.
14. Henry BM, Zwinczewska H, Roy J, Vikse J, Ramakrishnan PK, Walocha JA, Tomaszewski KA. The Prevalence of Anatomical Variations of the Median Nerve in the Carpal Tunnel: A Systematic Review and Meta-Analysis. PLoS One 2015;10:e0136477.
15. Hobson-Webb LD, Padua L. Ultrasound of Focal Neuropathies. J Clin Neurophysiol 2016;33:94-102.
16. Demircay E, Civelek E, Cansever T, Kabatas S, Yilmaz C. Anatomic variations of the median nerve in the carpal tunnel: a brief review of the literature. Turk Neurosurg 2011;21:388-96.
17. Benson LS, Bare AA, Nagle DJ, Harder VS, Williams CS, Visotsky JL. Complications of endoscopic and open carpal tunnel release. Arthroscopy 2006;22:919-24, 924.e1-2.
18. Palmer AK, Toivonen DA. Complications of endoscopic and open carpal tunnel release. J Hand Surg Am 1999;24:561-5.
19. Hanna A. Classification of the variations of the palmar recurrent branch of the median nerve with special emphasis on angulation. J Neurosurg 2020;133:556-63.
20. Poisel S. Ursprung und Verlauf des R. muscularis des Nervus digitals palmaris communis I (N. medianus). Chir Praxis 1974;18:471-4.
21. Lanz U. Anatomical variations of the median nerve in the carpal tunnel. J Hand Surg Am 1977;2:44-53.
22. Pivec C, Bodner G, Mayer JA, et al. Novel Demonstration of the Anterior Femoral Cutaneous Nerves using Ultrasound. Ultraschall Med 2018. [Epub ahead of print]. doi: 10.1055/s-0043-121628.
23. Basiri K, Katirji B. Practical approach to electrodiagnosis of the carpal tunnel syndrome: A review. Adv Biomed Res 2015;4:50.
24. Padua L, Cuccagna C, Giovannini S, Coraci D, Pelosi L, Loreti C, Bernabei R, Hobson-Webb LD. Carpal tunnel syndrome: updated evidence and new questions. Lancet Neurol 2023;22:255-67.
25. Mondelli M, Aretini A, Ginanneschi F, Padua L. Thenar motor neuropathy electrophysiological study of 28 cases. J Clin Neurophysiol 2010;27:344-9.
26. Lee CH, Kim CU. Delayed Repair of Severed Thenar Branch with Transligamentous Variation after Open Carpal Tunnel Release. J Hand Surg Asian Pac Vol 2019;24:494-7.
27. Chappell KE, Robson MD, Stonebridge-Foster A, Glover A, Allsop JM, Williams AD, Herlihy AH, Moss J, Gishen P, Bydder GM. Magic angle effects in MR neurography. AJNR Am J Neuroradiol 2004;25:431-40.
28. Filler A. Magnetic resonance neurography and diffusion tensor imaging: origins, history, and clinical impact of the first 50,000 cases with an assessment of efficacy and utility in a prospective 5000-patient study group. Neurosurgery 2009;65:A29-43.
29. Chang KJ, Kamel IR, Macura KJ, Bluemke DA. 3.0-T MR imaging of the abdomen: comparison with 1.5 T. Radiographics 2008;28:1983-98.
30. Choi JY, Kim MJ, Chung YE, Kim JY, Jones AC, de Becker J, van Cauteren M. Abdominal applications of 3.0-T MR imaging: comparative review versus a 1.5-T system. Radiographics 2008;28:e30.
31. Dos Santos Silva J, de Barros LFP, de Freitas Souza R, Mendonça SM, Costa FM, Landeiro JA, Lopes FCR, Acioly MA. "Million dollar nerve" magnetic resonance neurography: first normal and pathological findings. Eur Radiol 2022;32:1154-62.
32. Cambon-Binder A. Ulnar neuropathy at the elbow. Orthop Traumatol Surg Res 2021;107:102754.
33. Serhal A, Lee SK, Michalek J, Serhal M, Omar IM. Role of high-resolution ultrasound and magnetic resonance neurography in the evaluation of peripheral nerves in the upper extremity. J Ultrason 2023;23:e313-27.
34. Kalia V, Jacobson JA. Imaging of Peripheral Nerves of the Upper Extremity. Radiol Clin North Am 2019;57:1063-71.
35. Zaidman CM, Seelig MJ, Baker JC, Mackinnon SE, Pestronk A. Detection of peripheral nerve pathology: comparison of ultrasound and MRI. Neurology 2013;80:1634-40.
36. Picasso R, Zaottini F, Pistoia F, Perez MM, Klauser A, Rossi F, Schenone A, Tagliafico AS, Martinoli C. High-Resolution Ultrasound of Small Clinically Relevant Nerves Running Across the Posterior Triangle of the Neck. Semin Musculoskelet Radiol 2020;24:101-12.
37. Deshmukh S, Sun K, Komarraju A, Singer A, Wu JS.

Peripheral Nerve Imaging: Magnetic Resonance and Ultrasound Correlation. Magn Reson Imaging Clin N Am 2023;31:181-91.
38. Petrover D, Bellity J, Vigan M, Nizard R, Hakime A. Ultrasound imaging of the thenar motor branch of the median nerve: a cadaveric study. Eur Radiol 2017;27:4883-8.
39. Smith J, Barnes DE, Barnes KJ, Strakowski JA, Lachman N, Kakar S, Martinoli C. Sonographic Visualization of Thenar Motor Branch of the Median Nerve: A Cadaveric Validation Study. PM R 2017;9:159-69.
40. Riegler G, Pivec C, Platzgummer H, Lieba-Samal D, Brugger P, Jengojan S, Vierhapper M, Bodner G. High-resolution ultrasound visualization of the recurrent motor branch of the median nerve: normal and first pathological findings. Eur Radiol 2017;27:2941-9.
41. Picasso R, Zaottini F, Pistoia F, Beronio A, Bovis F, Hamedani M, Schenone A, Martinoli C. Recurrent motor branch neuropathy in carpal tunnel syndrome: An ultrasound study. Muscle Nerve 2023;68:184-90.
42. Mackinnon SE. Pathophysiology of nerve compression. Hand Clin 2002;18:231-41.
43. Upton AR, McComas AJ. The double crush in nerve entrapment syndromes. Lancet 1973;2:359-62.
44. Fiaschi P, Pacetti M, Secci F, Gennaro S. A rare case of first motor branch of median nerve schwannoma. Neurol Sci 2015;36:659-61.
45. Josty IC, Sykes PJ. An unusual schwannoma of the median nerve: effects on the motor branch. Br J Plast Surg 2001;54:71-3.
46. Squarzina PB, Adani R, Cerofolini E, Bagni A, Caroli A. Ancient schwannoma of the motor branch of the median nerve: a clinical case. Chir Organi Mov 1993;78:19-23.
47. Jensen TT. Isolated compression of the motor branch of the median nerve by a ganglion. Case report. Scand J Plast Reconstr Surg Hand Surg 1990;24:171.
48. Kato H, Ogino T, Nanbu T, Nakamura K. Compression neuropathy of the motor branch of the median nerve caused by palmar ganglion. J Hand Surg Am 1991;16:751-2.
49. Crowley B, Gschwind CR, Storey C. Selective motor neuropathy of the median nerve caused by a ganglion in the carpal tunnel. J Hand Surg Br 1998;23:611-2.
50. Widder S, Shons AR. Carpal tunnel syndrome associated with extra tunnel vascular compression of the median nerve motor branch. J Hand Surg Am 1988;13:926-7.
51. Yamanaka K, Horiuchi Y, Yabe Y. Compression neuropathy of the motor branch of the median nerve due to an anomalous thenar muscle. J Hand Surg Br 1994;19:711-2.
52. Ali E, Delamont RS, Jenkins D, Bland JD, Mills KR. Bilateral recurrent motor branch of median nerve neuropathy following long-distance cycling. Clin Neurophysiol 2013;124:1258-60.
53. Haussmann P. Isolated traumatic lesions of the motor nerve branches in the hand. Handchirurgie 1980;12:23-5.
54. Asghar A, Naaz S, Ansari S, Kumar A, Singh V. The cross-sectional morphology of median nerve in carpal tunnel of healthy, adult population: A systematic review and meta-analysis. Morphologie 2023;107:99-115.

Cite this article as: Wang Y, Chen W, Wang T, Qin K, Teng J, Qi H. Comparison of ultrasound and magnetic resonance imaging of the median nerve's recurrent motor branch and the value of its diameter in diagnosing carpal tunnel syndrome. Quant Imaging Med Surg 2025;15(1):383-394. doi: 10.21037/qims-24-1410